

A rapid route to carbazole containing dendrons and phosphorescent dendrimers†

Kevin A. Knights,^a Stuart G. Stevenson,^c Christopher P. Shipley,^a Shih-Chun Lo,^a Seth Olsen,^b Ruth E. Harding,^c Salvatore Gambino,^c Paul L. Burn^{*b} and Ifor D. W. Samuel^{*c}

Received 16th November 2007, Accepted 21st February 2008

First published as an Advance Article on the web 14th March 2008

DOI: 10.1039/b717750j

A convergent strategy for the synthesis of three generations of dendrons comprised of carbazole moieties is described. The procedure to build the dendrons involves an iterative palladium catalysed amination–debenzylation sequence using *N*-benzyl-3,6-dibromocarbazole. The three carbazolyl focussed dendrons are then attached to a reactive *fac*-tris[2-phenylpyridyl]iridium(III) core by a palladium catalysed amination to give the dendrimers. The three generations of dendrons have one, three, and seven carbazole units leading to dendrimers with *fac*-tris[2-phenylpyridyl]iridium(III) cores and three, nine and twenty one carbazole units. The use of 9,9'-dialkylfluorenyl surface groups gave the dendrimers excellent solubility. The attachment of the carbazolyl-based dendrons did not change the emission colour significantly with the dendrimers emitting green phosphorescence. The dendrimers were highly luminescent with solution photoluminescence quantum yields of the order of 70%. Ground state molecular orbital calculations showed that while the “LUMO” was concentrated on the core iridium(III) complex the “HOMO” was delocalised across the core and each of the dendrons. This was reflected in the oxidation properties of the dendrimers whereby the increased carbazolyl character of the “HOMO” resulted in the first oxidation being moved to more positive potentials.

Introduction

Phosphorescent complexes based on iridium(III) are likely to play an important role in bringing organic light-emitting diodes to market. In many cases the most efficient devices based on iridium(III) complexes have the complex blended with a host that is comprised of carbazole units.^{1–7} Phosphorescent complexes are sensitive to concentration quenching of the luminescence and hence one of the critical roles the host plays is to keep the emissive chromophores separated. However, while the guest–host composition may be well defined it is much more difficult to determine what the distribution and arrangement of the two components are in the deposited film. There is now a significant effort towards controlling the intermolecular interactions of iridium(III) complexes in the solid state by using dendritic architectures.^{8–13} Until recently the most efficient dendrimer based light-emitting diodes (DLEDs) had the light-emitting dendrimers blended with carbazole containing hosts^{14–17} although hostless dendrimer devices have now been reported,¹⁸ and the efficiencies of the devices have been found to be strongly dependent on the processing regime.¹⁹ What have been explored in less detail are dendritic materials that have the carbazolyl units normally found

in small molecule hosts incorporated into the dendrons to form a covalently linked guest–host system where the number of carbazolyl to emissive units is precisely known and the intermolecular interactions that govern the luminescence properties are controlled at a molecular level by the dendrimer generation.^{20–25} This has been in part due to the lack of efficient routes to higher generation carbazolyl containing dendrons. In addition, previous routes to phosphorescent dendrimers have generally involved the preparation of the dendronised ligand, which is subsequently reacted with an iridium(III) salt to give the dendrimer.^{23,24,26} These latter reactions can sometimes be low yielding.

In this paper we describe a simple iterative convergent procedure that rapidly leads to first, second, and third generation dendrons. We show that phosphorescent dendrimers with a *fac*-tris[2-phenylpyridyl]iridium(III) (Irppy₃) core can then be formed in a single step where the dendrons are reacted with an activated preformed complex. The third generation dendrimer has six mole percent (mol%) of (Irppy₃) core to carbazole units, which is similar to the most efficient small molecule devices with (Irppy₃) : 4,4'-bis(*N,N*-carbazolyl)biphenyl (CBP) blends (4.5 mol%). In addition, we report the optoelectronic properties of the dendrimers and relate these to their molecular orbital distribution.

Results and discussion

Synthesis

When developing the strategies for the preparation of dendrimers we have focussed on minimising the reaction types and steps for the formation of the different generations of

^aDepartment of Chemistry, University of Oxford, Chemistry Research Laboratory, Mansfield Rd, Oxford, UK OX1 3TA

^bCentre for Organic Photonics & Electronics, School of Molecular & Microbial Sciences, Chemistry Building, University of Queensland, St Lucia, Queensland, 4072, Australia

^cOrganic Semiconductor Centre, SUPA, School of Physics and Astronomy, University of St Andrews, St Andrews, Fife, UK KY16 9SS

† Electronic supplementary information (ESI) available: Cartesian coordinates of first, second and third generation dendrimer models. See DOI: 10.1039/b717750j

using tri-*tert*-butylphosphonium tetrafluoroborate gave more reliable yields than the simpler tri-*tert*-butylphosphine and that the benzyl-protected second generation dendron **5** could be formed in an 80% yield. Deprotection of **5** was achieved by treatment with aluminium chloride in anisole at 80 °C and under these conditions **6** was isolated in 51% yield. The cycle could be repeated to give the third generation benzyl-protected dendron **7** and deprotected material **8** in yields of 72% and 63% respectively. In the past we have normally taken the dendron and attached it to the ligand before complexation to the iridium(III). However, the formation of iridium complexes can be capricious so in this synthesis we have changed strategy. The final step in the synthesis of the three generations of dendrimers was the tris-dendronisation of the *fac*-tris[2-(3-bromophenyl)pyridyl]iridium(III) complex. The palladium catalysed aminations were carried out under the same conditions as for the dendron formation and the first (**9**), second (**10**), and third (**11**) generation materials were isolated in the respectable yields of 65%, 32% and 34%.

The ¹H NMR spectra of the dendrimers were found to be more complex than those of the dendrimers with biphenyl dendrons. In particular the aromatic region was complex with some of the signals, even for the first generation dendrimer, being broad, which may indicate hindered rotation due to steric encumbrance. The dendrimers were thermally stable to decomposition, for example, the first generation only showed significant weight loss above 385 °C. The hydrodynamic radii of the dendrimers were calculated from the \bar{M}_v s determined by gel permeation chromatography using polystyrene standards in combination with the Hester–Mitchell equation and Mark–Houwink relationship.³⁰ The first generation dendrimer had a hydrodynamic radius of 10.3 Å, which is similar to that of the first generation biphenyl dendrimer **12**.²⁶ It is interesting to note that in spite of the fact that the aromatic units in the carbazolyl dendrons of **9** are significantly larger than in the biphenyl dendrons of **12** the hydrodynamic radii are similar. This indicates that for the biphenyl-based dendrons the 2-ethylhexyloxy groups play an important role in controlling the intermolecular interactions of the emissive core. The second generation and third generation dendrimers, **10** and **11**, had hydrodynamic radii of 14.0 Å and 18 Å respectively; that is, the third generation has a hydrodynamic radius of almost twice that of the first. The three dendrimers were found to be monodisperse.

Molecular orbital calculations

Molecular orbital calculations in conjunction with experimental results can assist in understanding the optical and electronic properties of new materials. For example, in a previous study of a first generation Irppy₃-cored dendrimer with biphenyl based dendrons we calculated that the HOMO and LUMO of the dendrimer were strongly localised on the Irppy₃ core.²⁴ The fact that the orbital density was concentrated on the core complex was reflected in the difference in the photoluminescence and charge transporting properties of the first and second generation dendrimers. It was found that the second generation dendrimer was more photoluminescent in the solid state and that the hole mobility was lower. These two properties were consistent with the optically and electronically active cores being on average

held further apart by the larger dendrons in the second generation dendrimer.³¹ In contrast, it was found that when the branching moiety was changed from a phenyl group to a carbazolyl moiety the calculations showed that the HOMO was not only found on the Irppy₃ core but also on the carbazolyl units.²⁴ We were therefore interested to see how the molecular orbital distribution and energies correlated with the optical and electronic properties of the higher generation carbazole dendrimers.

The first part of the study was to calculate the molecular orbital distribution and energies (see Experimental section for details of the method). Given the size of the dendrimers and the concomitant complexity of the calculations we locked the angles between different aromatic units in the dendrons and their attachment points to the core at 30° to take into account the interactions between neighbouring aromatic units. Of course steric interactions could differ between different generations causing deviations from this structural arrangement, and hence only general trends should be drawn from the results. For example, if steric interactions caused larger twisting in the dendrons than allowed for in the calculations then the latter might give a slightly lower energy gap for the orbitals than is observed experimentally. Optimisation of a first generation model indicated a predilection for C₃ symmetry—calculations for higher generation models were performed within this symmetry group. We found that the HOMO and LUMO (belonging to the totally symmetric irreducible representation *A*) were close in energy to the HOMO – 1 and HOMO – 2, and LUMO + 1 and LUMO + 2 respectively (Fig. 1 illustrates the results for the third generation dendrimer **11**). The HOMO – 1 and HOMO – 2 belong to the *E* irreducible representation, as do the LUMO + 1 and LUMO + 2. Therefore, each orbital pair is degenerate within itself. The energy gap preceding the next lower and higher sets of orbitals (of *E* and *A* symmetry) is larger by about an order of magnitude; their influence is correspondingly less and it is reasonable not to consider them. The fact the first three HOMO and the first three LUMO orbitals are similar in energy means that the orbital distribution can be considered to be an average of these. Any asymmetric perturbation (for example, deviations from symmetric geometry or the effects of amorphous environments) will mix each triad within itself at lowest order. As can be seen in Fig. 1 the molecular orbital distribution of the “LUMO” (comprised of LUMO, LUMO + 1, and LUMO + 2) is strongly localised on the core complex, whereas the “HOMO” (comprised of HOMO, HOMO – 1, and HOMO – 2) has contributions from both the dendrons and the core complex. Similar results are observed for the first and second generation dendrimers.

We have analysed the molecular orbital distributions in more detail and the results for the first generation biphenyl **12** and carbazolyl dendronised dendrimers **9–11** are summarised in Table 1. In addition, Fig. 2 uses target diagrams to illustrate the distribution for dendrimers **9** and **12** to facilitate the explanation. For the first generation dendrimer with biphenyl-based dendrons **12** the LUMO density resides almost entirely on the 2-phenylpyridyl ligand (97%) with only around 2% on the iridium, and the remainder on the dendron. The LUMO distribution for the carbazolyl-dendronised dendrimers is essentially the same indicating that the carbazole units do not strongly affect the LUMO. As stated earlier the big difference between

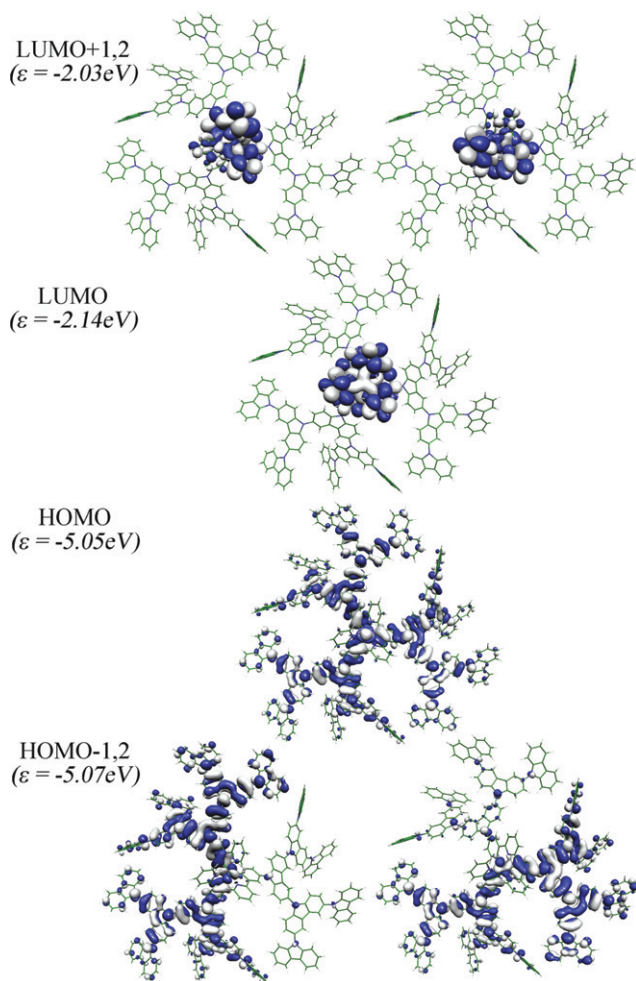


Fig. 1 Frontier orbitals in *A* and *E* symmetry for the third generation dendrimer **11**. The HOMO – 1 and HOMO – 2, and LUMO + 1 and LUMO + 2 are degenerate in energy.

the dendrimers with the biphenyl-dendronised dendrimers such as **12** and the carbazole containing materials is in the HOMO distribution. For **12** the HOMO distribution is similar to that for the simple complex with 53% of the density on the iridium, and 41% and 6% on the ligand and dendron respectively. That is, nearly all of the HOMO orbital density is on the central core metal complex. Moving to the first generation carbazole-dendronised dendrimer **9** the amount of HOMO density on the iridium is found to decrease to 25% with 34% on the

2-phenylpyridyl ligands. In contrast to **12**, where there was little HOMO density on the dendrons, for **9** there was 40% of the HOMO density on the first layer of carbazoyl units of the dendrons. For the second generation carbazoyl dendrimer **10** the HOMO distribution had even less on the iridium (10%) and ligand (21%) with most of the density now being found on the first (41%) and second (27%) layers of carbazole units. The dilution of the HOMO density on the iridium(III) complex continued with the third generation with only 9% found on the core complex with the remainder on the first (22%), second (38%), and third (31%) carbazole layers.

The fact that the HOMO is distributed over the whole of the carbazoyl dendronised dendrimers as opposed to being localised on the core complex suggests that the hole transport in the materials should be significantly different to the biphenyl dendronised dendrimers in which the HOMOs on adjacent cores are effectively isolated from one another. We have measured the hole mobility of **9** by the time-of-flight technique and obtain a value of $6 \times 10^{-5} \text{ cm}^2 \text{ V}^{-1} \text{ s}^{-1}$ at a field of 0.2 MV cm^{-1} . This contrasts with the hole mobility of $4 \times 10^{-6} \text{ cm}^2 \text{ V}^{-1} \text{ s}^{-1}$ measured at the same field for the first generation dendrimer **12**.³¹ The second and third generation carbazole dendrimers **10** and **11** have even higher mobilities than **9**. Therefore, the calculations give important insight into how the distribution of the molecular orbitals can lead to an understanding of the improved hole mobilities in films of the carbazole dendrimers, and how the carbazole units can enhance hole transport. We were also interested in seeing whether we could gain some insight into the nature of the optical properties of the dendrimers and hence carried out time dependent density functional theory (TD-DFT) calculations to determine the nature of the lowest energy excitations. For these calculations we used the same functional and basis sets as those used for determining the molecular orbital distributions. From these calculations it was found that the three lowest energy transitions for all three dendrimers, **9–11**, were triplet in nature. For the first generation dendrimer **9** the three lowest energies were 2.38, 2.41, and 2.44 eV, while for **10** and **11** they were 2.26, 2.28 and 2.29 eV, and 2.27, 2.29 and 2.30 eV respectively. The first point to note from these calculations is that the excitation energies for the three dendrimers are very similar. There is a slight red-shift in moving from the first to second generation but the second and third generation have similar energies. The TD-DFT calculations also show that the three lowest energy transitions are dominated by excitation combinations between the HOMO, HOMO – 1 and HOMO – 2, and LUMO, LUMO + 1 and LUMO + 2. That is, the

Table 1 Mulliken populations of the frontier molecular orbitals of the first generation biphenyl based dendrimer and the three generations of carbazoyl dendronised dendrimers. Ir = iridium(III), ppy = 2-phenylpyridyl ligand, Layer 1 = first level of carbazoyl or phenyl branching units, Layer 2 = second level of carbazoyl branching units, and Layer 3 = final level of carbazoyl units

Orbital	9		10		11		12	
	HOMO (%)	LUMO (%)	HOMO (%)	LUMO (%)	HOMO (%)	LUMO (%)	HOMO (%)	LUMO (%)
Ir	24.8	1.5	9.7	0.5	2.1	0.5	52.6	2.0
ppy	34.3	97.8	21.5	99.1	6.7	99.1	41.2	97.4
Layer 1	40.4	0.3	41.5	0.4	22.3	0.4	6.2	0.3
Layer 2			27.3	0.0	37.8	0.01		
Layer 3					31.1	0.0		

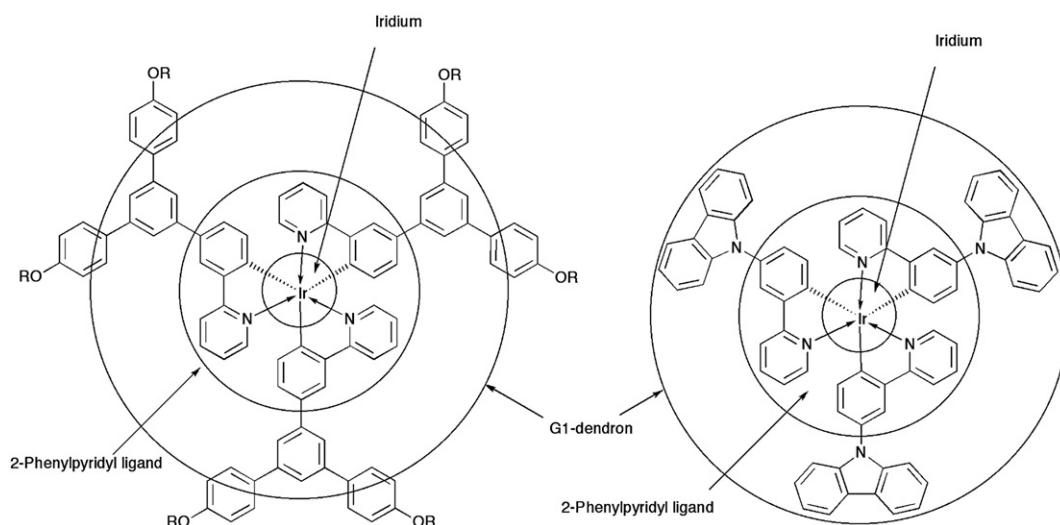


Fig. 2 ‘Targets’ showing the divisions of the Mulliken populations of the frontier molecular orbitals for the first generation biphenyl **12** (R = 2-ethyl-hexyl) and carbazoyl **9** dendrimers used in the generation of Table 1. The percentages shown in Table 1 arise from the orbital populations in the area between a given circle and the next inward circle. The fluorenyl surface groups for the carbazoyl dendrimers have been omitted to enable a simpler calculation.

excitations are not strictly metal–ligand charge transfer transitions as the “HOMO” has iridium metal, ligand, and carbazole dendron character. However, care needs to be taken in not over-interpreting these energies with regard to the excitation and light emission properties of the dendrimers as they are based on their ground state geometries.

Photophysical properties

The solution UV-visible spectra of the iridium(III) complex-cored dendrimers of **9**, **10**, **11**, and **12** are shown in Fig. 3. The UV-visible spectra of such dendrimers are comprised of two components.^{24,26} The short wavelength component is due to the π – π^* absorptions of the dendrons and ligand while the longer wavelength weak absorptions are due to the nominally metal-

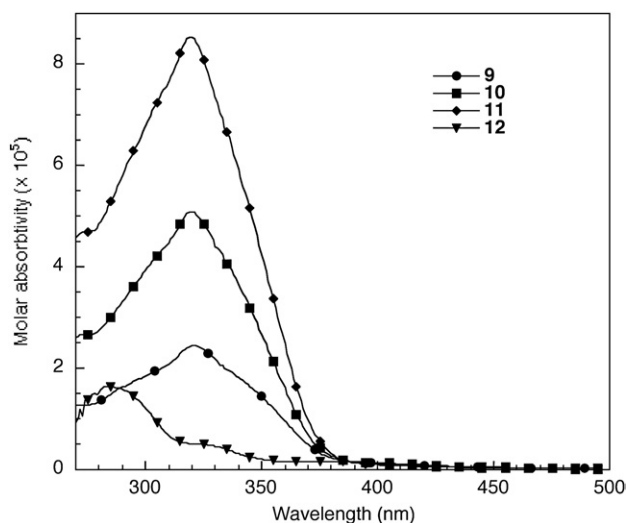


Fig. 3 Solution UV-visible spectra of **9**, **10**, **11**, and **12**. **9**, **10**, and **11** were measured in dichloromethane while **12** was a solution in toluene.

to-ligand charge transfer states. In comparison to **12** the carbazole containing dendrimers have strong π – π^* absorptions at longer wavelengths and this is due to the fact that the carbazoyl units have a smaller HOMO–LUMO energy gap than phenyl rings. As expected the absorption at 320 nm, which is due primarily to the carbazoyl units, increased with generation, that is, with number of carbazole units. Due to the large oscillator strength and number of chromophores with π – π^* absorptions the absorptions involving the iridium(III) are swamped for the carbazoyl containing dendrimers (the extinction coefficients are summarised in the Experimental section). It should be noted that the similarity in the lowest excitation energy determined from the TD-DFT calculations is reflected in the solution absorption spectra which all have shoulders at around 480 nm.

The next stage in understanding the photophysical properties of the dendrimers was the determination of the effect of the carbazoyl dendrons on the photoluminescence properties of the dendrimers. The solution photoluminescence (PL) spectra of the dendrimers are shown in Fig. 4. It can be seen in Fig. 4 there are only slight differences in the PL maxima with **12** having a maximum at 514 nm²⁶ with **9**–**11** having maxima in the range 510–524 nm, that is, the dendrimers emit green light. The fact that there is not a red-shift in the emission spectrum in moving from the first to the second and third generation dendrimers seems at first to contradict the calculations of the energies of the lowest transitions. However, it should be noted that to simplify the calculations we set the angles between the carbazoyl units at 30°, and if the angles were larger then the delocalisation would be reduced with the emission occurring at shorter wavelengths. Alternatively the PL spectra provides some evidence that calculation of the excitation energies based on a ground state geometry may not be a good method for understanding the emissive properties of these materials. That is, the excited state geometry may be significantly different from the ground state particularly if the symmetry is broken. The view that the ground and excited state geometries are different is strengthened

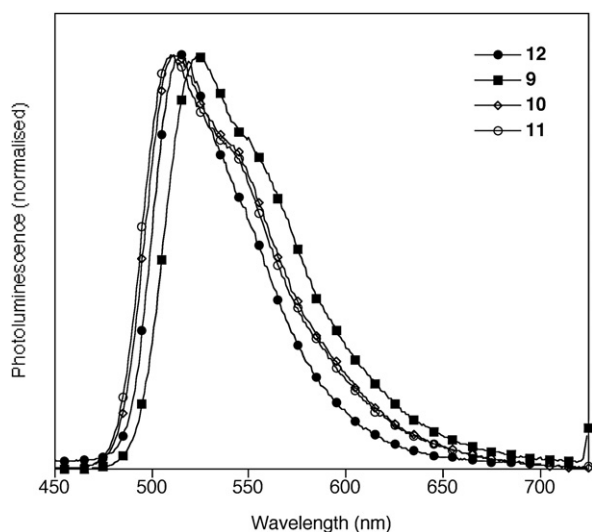


Fig. 4 Solution photoluminescence spectra of **9**, **10**, **11**, and **12**.

by time resolved PL measurements, which showed that the radiative decay rates of the carbazole dendronised dendrimers were around $5.6 \times 10^5 \text{ s}^{-1}$.³² If the emissive state had more dendron character then this would correspond to greater p-orbital triplet character and hence slower radiative rate than the simple complex should be observed. This is not the case as Irppy₃ has a very similar radiative decay rate of $6.7 \times 10^5 \text{ s}^{-1}$.³³ The computation of the excited state geometries is a challenging task with the current methodologies. The final step in the photo-physical study was the measurement of the solution PL quantum yields (PLQY) to determine whether the addition of the carbazolyl dendrons was detrimental to the luminosity of the materials. **12** has been reported to have a PLQY of 70%³³ and **9**, **10**, and **11** have PLQYs of 75%, 68%, and 66% respectively. Clearly these results show that the carbazolyl dendrons do not appreciably quench the luminescence of the core.

Electrochemistry

The oxidation properties of the dendrimers were studied by cyclic voltammetry at a scan rate of 50 mV s^{-1} . The Irppy₃ complex that is at the core of the dendrimers undergoes one oxidative process with an $E_{1/2}$ of 0.26 V being reported.³⁴ Dendrimer **12** with biphenyl dendrons attached to the Irppy₃ core also has a single oxidative process with the $E_{1/2}$ being 0.24 V.²⁶ This indicates that the oxidation of dendrimer **12** occurs essentially on the iridium(III) complex at the core and is consistent with the calculations of the molecular orbital calculations that shows the HOMO of **12** is essentially on the complex. In contrast the first generation carbazolyl dendrimer **9** has three clearly defined chemically reversible oxidations at 0.29 V, 0.57, and 0.73 V, and an ill-defined process at more positive potentials (Fig. 5). The fourth oxidation can be resolved using differential pulse voltammetry (DPV). On moving to the second generation dendrimer **10** the first oxidation process is seen to move to a more positive potential with an $E_{1/2}$ of 0.36 V with the second oxidation having an apparent $E_{1/2}$ of 0.56 V. There is also a third oxidation process that occurs at a similar position to the first generation carbazole dendrimer **9**. At first glance the third

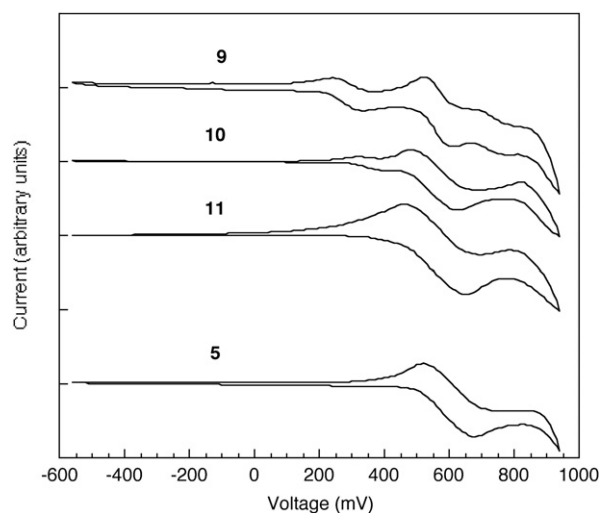


Fig. 5 Cyclic voltammograms of **9**, **10**, **11**, and **5**. The voltammograms have been offset for clarity. All the oxidation potentials are quoted against the ferricenium/ferrocene couple.

generation dendrimer appears to have only one oxidation process with an E_{pa} of 0.65 V and an E_{pc} of 0.45 V.

The first point to note from the electrochemistry is that there appears to be a trend for the first oxidation to move to more positive potentials: 0.29 V for **9** and 0.36 V for **10**. Close examination of the onset to the oxidation process(es) for **11** shows that it is less steep for **11** than **9** and **10** hinting that there is another process occurring that is not resolved under the experimental conditions. DPV was only partially successful in resolving the first oxidation from the latter processes but a shoulder on the main oxidation peak could be seen clearly. From the DPV it was estimated that the first oxidation of **11** was at $\approx 0.42 \text{ V}$, a further shift to more positive potentials. An explanation for the shift to more positive potentials for the first oxidative process with increasing generation is that while for **12** the oxidation is predominantly an Irppy₃ complex based process for **9–11** the first oxidation has carbazolyl character. The molecular orbital calculations show that the carbazolyl character increases from the first to the third generation dendrimer and so the oxidation potential which is partly comprised of the core complex should move closer to those of the carbazolyl units. The oxidation cyclic voltammogram of the second generation benzyl protected dendron **5** is also shown in Fig. 5. It can be seen that its oxidations occur at similar potentials to that of the second oxidations of **9** and **10**, and the oxidation of **11**. Given that the only redox active moieties in **5** are the carbazole units then the latter oxidations in the dendrimers could be significantly dendron based. This view is strengthened by the electrochemical results for the second and third generation dendrimers where there are a series of overlapping oxidations rather than just a single oxidative process. Evidence for this comes from the fact that the difference between the E_{pa} and E_{pc} is larger for the higher generation dendrimers (150–200 mV) than for the first generation dendrimer ($\approx 95 \text{ mV}$) even though the scan rates are the same. This makes sense as the higher generation dendron **5** and dendrimers **10** and **11** all have carbazole units that are in slightly different environments and hence different oxidation potentials.

Conclusion

We report a new simple strategy for preparing carbazolyl-based dendrons of different generations. The key to the strategy is that there is a simple iterative two-step procedure, namely a palladium catalysed amination followed by a benzyl deprotection. The dendrimers containing a *fac*-tris[2-phenylpyridyl]iridium(III) complex core were also prepared by a new method involving the attachment of the dendrons to a preformed tris-brominated complex again using palladium catalysis. This meant that the third generation dendrimer could be prepared in six simple steps. While it was found that the attachment of the carbazolyl dendrons did not affect the photoluminescence properties of the dendrimers with respect to those with the same core but biphenyl based dendrons, molecular orbital calculations on the carbazolyl containing dendrimers indicated that the "HOMO" was not just located on the core but also over the carbazolyl units in the dendrons. The delocalized HOMO has the effect of increasing the hole-transport properties of the dendrimers and this will be reported in detail elsewhere.

Experimental

Measurements

NMR spectra were recorded on Bruker DPX400, DQX400, or AVII500 spectrometers: CarbH = carbazole H, LigH = ligand H, and FIH = fluorenyl H. All *J* values are in Hertz and are rounded to the nearest 0.5 Hz. UV-visible spectra were recorded on a Perkin-Elmer UV-visible Lambda 25 spectrometer and were recorded as solutions in spectroscopic grade dichloromethane. Infrared spectra were recorded on a Perkin Elmer Spectrum 1000 FT-IR or a Brüker Tensor 27 FT-IR spectrometer. Mass spectra were recorded on an Applied Biosystems Voyager matrix-assisted laser desorption/ionisation time-of-flight (MALDI-TOF) from 2-[(2*E*)-3-(4-*tert*-butylphenyl)-2-methylprop-2-enylidene]malononitrile (DCTB) in positive reflectron mode, or positive linear mode for **11**, at the EPSRC National Mass Spectrometry Centre, Swansea, UK, or a VG AutoSpec for CI. Melting points were recorded on a Gallenkamp or a Leica Galen III melting point apparatus and are uncorrected. Microanalyses were carried out in the Inorganic Chemistry Laboratory, Oxford or at London Metropolitan University, UK. Gel permeation chromatography (GPC) was carried out using PLgel Mixed-A columns (600 mm + 300 mm lengths, 7.5 mm diameter) from Polymer Laboratories calibrated with polystyrene narrow standards ($\bar{M}_p = 580$ to 3.2×10^6) in tetrahydrofuran with toluene as flow marker. The tetrahydrofuran was degassed with helium and pumped with a rate of $1 \text{ cm}^3 \text{ min}^{-1}$ at $30.0 \text{ }^\circ\text{C}$. Thermal gravimetric analysis was performed on a Perkin Elmer Thermogravimetric Analyzer TGA 7. Light petroleum refers to the fraction of boiling point $40\text{--}60 \text{ }^\circ\text{C}$. When solvent mixtures are used for chromatography over silica the proportions are given by volume. All solvents used were of HPLC or Analar grade. Tetrahydrofuran was dried by distillation from sodium benzophenone ketal or by passage through activated alumina. Xylene and toluene were dried by distillation from calcium hydride.

Electrochemistry was performed using an EG&G Princeton Applied Research potentiostat/galvanostat model 263A using

platinum working, Ag/AgCl/NaCl reference, and platinum counter electrodes, and a 50 mV s^{-1} scan rate. All measurements were made at room temperature on samples at a 1 mM concentration in dichloromethane, with 0.1 M tetra-*n*-butylammonium tetrafluoroborate as the electrolyte. HPLC grade dichloromethane was used for the oxidation studies. The solutions were deoxygenated with argon and the ferrocenium/ferrocene couple was used as standard.³⁵ In all cases several scans were carried out to confirm the chemical reversibility of the redox processes.

Solution PLQYs were measured by a relative method using quinine sulfate in 0.5 M sulfuric acid, which has a PLQY of 54.6%, as the standard.³⁶ The dendrimers were dissolved in tetrahydrofuran and freeze-thaw degassed. Photoluminescence spectra were recorded in a JY Horiba Fluoromax 2 fluorimeter, with the dendrimer solutions excited at 360 nm . The optical densities of the standard and sample were similar and small (less than/equal to 0.1). The accuracy of these measurements is estimated to be $\pm 10\%$ of the stated value. The time-resolved luminescence measurements were performed using the time-correlated single photon counting technique, with excitation at 390 nm from a pulsed gallium nitride laser. The hole mobility was measured using the charge generation layer time-of-flight method. Dendrimer films $200\text{--}300 \text{ nm}$ thick were prepared by spin-coating, and a 10 nm lumogen red charge injection layer evaporated on top of them. The sample was excited by a nitrogen pumped dye laser at 580 nm .

Density functional theory (DFT) calculations were performed in C_3 symmetry using the Gaussian 03 suite of programs³⁷ with a LanL2DZ basis set³⁸⁻⁴¹ and B3LYP level of theory⁴² Geometries were optimised structures with the pendant phenyl and carbazole units held at 30° to the ligand phenyl or ring bearing them. Compositions of molecular orbitals were calculated using the AOMix Program.^{43,44} Linear response TD-DFT calculations of the 6 lowest states of singlet and triplet character were performed within the random phase approximation using the same functional and basis set. The Cartesian co-ordinates of the models (in Å) are provided in the ESI.† Although the theoretical foundations which underlie the use of Kohn-Sham orbitals in chemical analyses are less rigorous than those for, *e.g.*, Hartree-Fock canonical orbitals, they have been found empirically to give useful orbital energies⁴⁵ and singlet-triplet excitation splittings.⁴⁶

3,6-(Bis[9,9'-di-*n*-propylfluoren-2-yl])carbazole 3

3,6-Dibromocarbazole **2** (9.03 g, 27.8 mmol) and 9,9'-di-*n*-propylfluorenyl-2-boronic acid **1** (19.9 g, 67.8 mmol) were dissolved in toluene (75 cm^3) and ethanol (59 cm^3). Aqueous sodium carbonate (2 M , 75 cm^3) was added, and the mixture was deoxygenated with argon for 5 min. The mixture was heated to $100 \text{ }^\circ\text{C}$ and tetrakis(triphenylphosphino)palladium(0) (1.77 g, 1.53 g) was added and then the reaction was heated at $100 \text{ }^\circ\text{C}$ for a further 23 h. The mixture was allowed to cool to room temperature and water (200 cm^3) was added. The organic layer was separated and the aqueous layer was extracted with ether ($2 \times 200 \text{ cm}^3$). The combined organic layers were washed with brine (200 cm^3), dried over anhydrous magnesium sulfate, filtered, and the solvent was removed. The residue was purified in three stages: first, it was passed through a silica plug using

a dichloromethane : light petroleum mixture (1 : 1) as eluent; second, it was purified by column chromatography over silica using a dichloromethane : light petroleum mixture (1 : 4 to 3 : 7) as eluent; and finally, it was recrystallised from a dichloromethane : methanol mixture to give **3** (14.05 g, 76%): mp 229–230 °C (Found: C, 90.3%; H, 7.5%; N, 2.1%. C₅₀H₄₉N requires C, 90.45%; H, 7.4%; N, 2.1%); ν_{\max} (KBr) 3396 cm⁻¹ (NH); λ_{\max} (CH₂Cl₂) 269 nm (log ϵ /dm³ mol⁻¹ cm⁻¹ 4.49), 319 (4.89), 399sh (4.77); δ_{H} (400 MHz, CDCl₃) 0.70–0.85 (20 H, m, CH₂CH₃ and CH₃), 2.00–2.10 (8 H, m, CH₂CH₂CH₃), 7.30–7.42 (6 H, m, CarbH and/or FIH), 7.57 (2 H, d, *J* = 8, CarbH), 7.70–7.85 (10 H, m, CarbH and/or FIH), 8.17 (1 H, bs, NH), 8.48 (2 H, s, CarbH); *m/z* (CI, NH₃) 664 [MH]⁺ (100%).

***N*-Benzyl-3,6-bis[3,6-bis(9,9'-di-*n*-propylfluoren-2-yl)carbazolyl]carbazole 5**

N-Benzyl-3,6-dibromocarbazole **4** (1.97 g, 4.75 mmol), **3** (7.07 g, 10.6 mmol), sodium *tert*-butoxide (1.92 g, 20.0 mmol) and tri-*tert*-butylphosphonium tetrafluoroborate (506 mg, 1.74 μ mol) were placed into a pressure tube fitted with a Young's valve and deoxygenated by placing under vacuum and back filling with nitrogen. Mixed xylenes (30 cm³) were added and the resultant solution deoxygenated three times. Tris(dibenzylideneacetone)dipalladium(0) (200 mg, 218 μ mol) was added, the solution was deoxygenated three times and the tube was sealed and heated at 135 °C for 17 h. The mixture was cooled and filtered through a silica plug using dichloromethane as eluent. The filtrate was collected and the solvent removed. The crude product was purified by flash chromatography over silica using a dichloromethane : light petroleum mixture (1 : 4 to 7 : 13) to give a mixture of **5** and **3**. The mixture was adsorbed onto silica and **3** was removed by elution with a 2-propanol : light petrol mixture (1 : 9). After removal of **3**, elution with dichloromethane gave **5** as a white solid (6.00 g, 80%): mp 263–265 °C (Found: C, 90.4%; H, 6.9%; N, 2.6%. C₁₁₉H₁₀₉N₃ requires C, 90.4%; H, 6.95%; N, 2.7%); λ_{\max} (CH₂Cl₂) 272 nm (log ϵ /dm³ mol⁻¹ cm⁻¹ 4.87), 302sh (5.09), 321 (5.22), 342sh (5.06); δ_{H} (400 MHz, CD₂Cl₂) 0.70–0.85 (40 H, m, CH₂CH₃ and CH₃), 2.02–2.18 (16 H, m, CH₂CH₂CH₃), 5.84 (2 H, s, CH₂Ph), 7.33–7.50 (17 H, m, CarbH and/or FIH, and PhH), 7.60 (4 H, d, *J* = 8.5, CarbH), 7.76–7.88 (24 H, m, CarbH and/or FIH), 8.46 (2 H, s, CarbH), 8.52 (4 H, s, CarbH); *m/z* (MALDI-TOF) Anal. Calcd for C₁₈₃H₁₆₅IrN₆: 2637.3 (21%), 2638.3 (41%), 2639.3 (78%), 2640.3 (100%), 2641.3 (89%), 2642.3 (55%), 2643.3 (27%), 2644.3 (12%), 2645.3 (6%), 2646.3 (2%). Found: 2637.3 (32%), 2638.3 (56%), 2639.3 (89%), 2640.3 (100%), 2641.3 (89%), 2642.3 (64%), 2643.3 (30%), 2644.3 (11%), 2645.3 (5%), 2646.3 (2%) (M⁺).

3,6-Bis[3,6-bis(9,9'-di-*n*-propylfluoren-2-yl)carbazolyl]carbazole 6

5 (4.26 g, 2.69 mmol) was dissolved in anisole (250 cm³). Aluminium chloride (17.00 g, 128 mmol) was added, and the mixture heated at 90 °C overnight. After cooling, methanol (20 cm³) was added and the mixture was passed through a plug of silica using dichloromethane as eluent. The solvent was removed and the residue was purified by column

chromatography over silica using a dichloromethane : light petroleum mixture (1 : 3 to 2 : 5) as eluent to give **6** as a white powder (2.06 g, 51%): mp 238–240 °C (Found: C, 89.8%; H, 7.2%; N, 2.7%. C₁₁₂H₁₀₃N₃ requires C, 90.2%; H, 7.0%; N, 2.8%); ν_{\max} (KBr) 3408 cm⁻¹ (NH); λ_{\max} (CH₂Cl₂) 272 nm (log ϵ /dm³ mol⁻¹ cm⁻¹ 4.85), 302sh (5.09), 321 (5.22), 342sh (5.08); δ_{H} (400 MHz, CDCl₃) 0.67–0.83 (40 H, m, CH₂CH₃ and CH₂CH₃), 2.00–2.15 (16 H, m, CH₂CH₂CH₃), 7.31–7.45 (12 H, m, CarbH and/or FIH), 7.56 (4 H, d, *J* = 8, CarbH), 7.70–7.85 (24 H, m, CarbH and/or FIH), 8.36 (2 H, s, CarbH), 8.53 (1 H, s, NH), 8.58 (4 H, s, CarbH); *m/z* [MALDI-TOF] Anal. Calcd for C₁₁₂H₁₀₃N₃: 1489.8 (79%), 1490.8 (100%), 1491.8 (64%), 1492.8 (26%), 1493.8 (7%), 1494.8 (2%). Found: 1489.8 (86%), 1490.8 (100%), 1491.8 (55%), 1492.9 (33%), 1493.9 (9%), 1494.9 (2%) (M⁺).

***N*-Benzyl-3,6-bis[3,6-bis(3,6-bis(9,9'-di-*n*-propylfluoren-2-yl)carbazolyl)carbazolyl]carbazole 7**

4 (415 mg, 1.00 mmol), **6** (3.50 g, 2.35 mmol), sodium *tert*-butoxide (497 mg, 5.18 mmol) and tri-*tert*-butylphosphonium tetrafluoroborate (300 mg, 1.03 mmol) were placed into a pressure tube fitted with a Young's valve and deoxygenated by placing under vacuum and then back filling with nitrogen. Mixed xylenes (25 cm³) were added and the resultant solution deoxygenated five times. Tris(dibenzylideneacetone)dipalladium(0) (120 mg, 130 μ mol) was added, the solution was deoxygenated three times and the tube was sealed and heated at 130 °C for 14 h. The mixture was cooled and filtered through a silica plug using dichloromethane as eluent. The filtrate was collected and the solvent removed. The residue was purified by flash chromatography over silica using a dichloromethane : light petroleum mixture (3 : 7 to 2 : 5) as eluent to give **7** as a white solid (2.35 g, 73%): mp >280 °C (Found: C, 90.0%; H, 6.9%; N, 2.85%. C₂₄₃H₂₁₇N₇ requires C, 90.2%; H, 6.8%; N, 3.0%); λ_{\max} (CH₂Cl₂) 272 nm (log ϵ /dm³ mol⁻¹ cm⁻¹ 5.19), 304sh (5.41), 320 (5.52), 343sh (5.35); δ_{H} (500 MHz, CDCl₃) 0.69–0.88 (80 H, m, CH₂CH₃ and CH₃), 2.00–2.16 (32 H, m, CH₂CH₂CH₃), 5.90 (2 H, s, CH₂Ph), 7.31–7.43 (24 H, m, CarbH and/or FIH), 7.46–7.56 (5 H, m, PhH), 7.60 (8 H, d, *J* = 8.5, CarbH), 7.73–7.87 (48 H, m, CarbH and/or FIH), 7.89–8.01 (4 H, m, CarbH and/or FIH), 8.49 (4 H, s, CarbH), 8.59 (8 H, s, CarbH), 8.69 (2 H, s, CarbH); *m/z* [MALDI-TOF] Anal. Calcd for C₂₄₃H₂₁₇N₇: 3232.7 (27%), 3233.7 (73%), 3234.7 (100%), 3235.7 (91%), 3236.7 (60%), 3237.7 (34%), 3238.7 (16%), 3239.7 (5%), 3240.7 (3%). Found: 3232.7 (43%), 3233.7 (90%), 3234.7 (98%), 3235.7 (100%), 3236.7 (68%), 3237.7 (33%), 3238.7 (17%), 3239.7 (5%), 3240.7 (3%) (M⁺).

3,6-Bis[3,6-bis(3,6-bis(9,9'-di-*n*-propylfluoren-2-yl)carbazolyl)carbazolyl]carbazole 8

7 (1.01 g, 312 μ mol) and aluminium chloride (5.00 g, 38 mmol) were dissolved in anisole and heated at 90 °C for 2 h. After cooling, the reaction was quenched with water (50 cm³). Ether (50 cm³) and dilute hydrochloric acid (3 M, 50 cm³) were added and the layers were separated. The organic layer was washed with water (50 cm³) and brine (50 cm³), dried over magnesium sulfate and filtered before the solvent was removed. The crude

material was purified by column chromatography over silica using a dichloromethane : light petroleum mixture (3 : 7 to 1 : 1) as eluent to give **8** as a white solid (0.61 g, 62%): mp >280 °C (Found: C, 89.8%; H, 6.5%; N, 2.95%. $C_{236}H_{210}N_7$ requires C, 90.1%; H, 6.8%; N, 3.1%); ν_{\max} (KBr) 3413 cm^{-1} (NH); λ_{\max} (CH_2Cl_2) 272 nm (log $\epsilon/dm^3 mol^{-1} cm^{-1}$ 5.17), 304sh (5.40), 320 (5.51), 342sh (5.36); δ_H (500 MHz, $CDCl_3$) 0.68–0.87 (80 H, m, CH_2CH_3 and CH_3), 2.00–2.14 (32 H, m, $CH_2CH_2CH_3$), 7.33–7.55 (24 H, m, CarbH and/or FIH), 7.60 (8 H, d, $J = 8.5$, CarbH), 7.72–7.85 (48 H, m, CarbH and/or FIH), 7.95 (4 H, m, CarbH and FIH), 8.47 (4 H, s, CarbH), 8.57 (8 H, s, CarbH), 8.61 (2 H, s, CarbH), 8.71 (1 H, s, NH); m/z [MALDI-TOF] Anal. Calcd for $C_{236}H_{211}N_7$: 3142.7 (27%), 3143.7 (75%), 3144.7 (100%), 3145.7 (88%), 3146.7 (57%), 3147.7 (28%), 3148.7 (14%), 3149.7 (5%), 3150.7 (2%). Found: 3142.7 (34%), 3143.7 (84%), 3144.7 (100%), 3145.7 (86%), 3146.7 (53%), 3147.7 (26%), 3148.7 (13%), 3149.7 (5%), 3150.7 (2%) (M^+).

***fac*-Tris[2-(3-{3,6-bis(9,9'-di-*n*-propylfluoren-2-yl)carbazoyl}phenyl)pyridyl]iridium(III)**

A mixture of *fac*-tris[2-(3-bromophenyl)pyridyl]iridium(III)⁴⁷ (383 mg, 439 μ mol), **3** (1.00 g, 1.51 mmol), sodium *tert*-butoxide (192 mg, 2.00 mmol) and tri-*tert*-butylphosphonium tetrafluoroborate (100 mg, 345 μ mol) was placed into a pressure tube fitted with a Young's valve and deoxygenated by placing under vacuum and backfilling with nitrogen. Toluene (10 cm^3) was added and the resultant solution deoxygenated by placing under vacuum and filling with nitrogen three times. Tris(dibenzylideneacetone)dipalladium(0) (40 mg, 44 μ mol) was added, and the solution deoxygenated by placing under vacuum and filling with nitrogen three times. The tube was sealed and the reaction mixture was heated at 110 °C for 17 h. The mixture was cooled and then filtered through a plug of silica using dichloromethane as eluent. To this solution was added silica and then the solvent was removed. The preloaded silica was added onto a silica chromatography column packed with light petroleum and a light petroleum : 2-propanol solvent mixture (4 : 1) was used to elute the majority of the free carbazole and then dichloromethane was used to elute crude **9**. Crude **9** was further purified by column chromatography over silica using a dichloromethane : light petroleum mixture (3 : 7 to 7 : 13) as eluent to give **9** as a yellow powder (759 mg, 65%): mp >280 °C (Found: C, 83.2%; H, 6.3%; N, 3.2%. $C_{183}H_{165}IrN_6$ requires C, 83.2%; H, 6.3%; N, 3.2%); λ_{\max} (CH_2Cl_2) 271 nm (log $\epsilon/dm^3 mol^{-1} cm^{-1}$ 5.10), 307sh (5.31), 320 (5.39), 336sh (5.29), 401sh (4.29), 438sh (3.88), 480sh (3.43); δ_H (400 MHz, C_6D_6) 0.77 (36 H, t, $J = 7$, CH_3), 0.89–1.11 (24 H, m, CH_2CH_3), 2.00–2.19 (24 H, m, $CH_2CH_2CH_3$), 6.36 (3 H, dd, $J = 6.5$, $J = 6.5$, LigH), 6.94 (3 H, dd, $J = 8$, $J = 8$, LigH), 7.11–8.11 (69 H, m, LigH, CarbH, FIH), 8.79 (2 H, s, CarbH); m/z [MALDI-TOF] Anal. Calcd for $C_{183}H_{165}IrN_6$: 2637.3 (21%), 2638.3 (41%), 2639.3 (78%), 2640.3 (100%), 2641.3 (89%), 2642.3 (55%), 2643.3 (27%), 2644.3 (12%), 2645.3 (6%), 2646.3 (2%). Found: 2637.3 (32%), 2638.3 (56%), 2639.3 (89%), 2640.3 (100%), 2641.3 (89%), 2642.3 (64%), 2643.3 (30%), 2644.3 (11%), 2645.3 (5%), 2646.3 (2%) (M^+); GPC: $\bar{M}_w = 2334$, $\bar{M}_v = 2294$, Polydispersity (PD) = 1.1.

***fac*-Tris[2-(3-{3,6-bis[3,6-bis(9,9'-di-*n*-propylfluoren-2-yl)carbazoyl]carbazoyl}phenyl)pyridyl]iridium(III)**

A mixture of *fac*-tris[2-(3-bromophenyl)pyridyl]iridium(III) (150 mg, 168 μ mol), **6** (0.95 g, 0.64 mmol), sodium *tert*-butoxide (140 mg, 1.46 mmol) and tri-*tert*-butylphosphonium tetrafluoroborate (176 mg, 0.61 mmol) was placed into a pressure tube fitted with a Young's valve and degassed. Mixed xylenes (10 cm^3) were added and the resultant solution was deoxygenated by placing under vacuum and backfilling with nitrogen three times. Tris(dibenzylideneacetone)dipalladium(0) (70 mg, 76 μ mol) was added, the solution was deoxygenated by placing under vacuum and backfilling with nitrogen a further three times, and then heated at reflux for 3 days. The mixture was cooled, filtered through a plug of silica using dichloromethane as eluent, and then the filtrate was collected and the solution removed. The residue was purified by column chromatography over silica in two steps: first using a dichloromethane : light petroleum mixture (2 : 3) as eluent and then by using a benzene : light petroleum mixture (3 : 2) as eluent to give **10** as a yellow powder (274 mg, 32%): mp >280 °C (Found: C, 86.4%; H, 6.5%; N, 3.2%. $C_{369}H_{327}IrN_{12}$ requires C, 86.5%; H, 6.4%; N, 3.3%); λ_{\max} (CH_2Cl_2) 273 nm (log $\epsilon/dm^3 mol^{-1} cm^{-1}$ 5.43), 306sh (5.63), 320 (5.71), 400sh (4.10), 440sh, (3.66) 480sh (3.22); δ_H (400 MHz, C_6D_6) 0.74 (72 H, t, $J = 7.5$, CH_3), 0.90–1.10 (48 H, m, CH_2CH_3), 2.00–2.17 (48 H, m, $CH_2CH_2CH_3$), 6.44 (3 H, dd, $J = 8$, $J = 8$, LigH), 7.04 (3 H, dd, $J = 8.5$, $J = 8.5$, LigH), 7.31–8.32 (141 H, m, LigH, CarbH, FIH), 8.82 (12 H, s, CarbH); m/z [MALDI-TOF] Anal. Calcd for $C_{369}H_{327}IrN_{12}$: 5116.6 (4%), 5117.6 (13%), 5118.6 (33%), 5119.6 (62%), 5120.6 (87%), 5121.6 (100%), 5122.6 (88%), 5123.6 (71%), 5124.6 (43%), 5125.6 (28%), 5126.6 (12%), 5127.6 (6%), 5128.6 (3%). Found: 5116.5 (5%), 5117.5 (17%), 5118.5 (44%), 5119.5 (69%), 5120.5 (93%), 5121.5 (100%), 5122.5 (90%), 5123.5 (66%), 5124.5 (43%), 5125.5 (23%), 5126.5 (8%), 5127.5 (5%), 5128.5 (3%) (M^+). GPC: $\bar{M}_w = 3995$, $\bar{M}_v = 3921$, PD = 1.15

***fac*-Tris[2-(3-{3,6-bis[3,6-bis(3,6-bis(9,9'-di-*n*-propylfluoren-2-yl)carbazoyl]carbazoyl}phenyl)pyridyl]iridium(III)**

A mixture of *fac*-tris[2-(3-bromophenyl)pyridyl]iridium(III) (36 mg, 40 μ mol), **8** (578 mg, 184 μ mol), sodium *tert*-butoxide (75 mg, 0.78 mmol) and tri-*tert*-butylphosphonium tetrafluoroborate (64 mg, 0.22 mmol) was placed into a pressure tube fitted with a Young's valve and deoxygenated by placing under vacuum and backfilling with nitrogen. Toluene (10 cm^3) was added and the resultant solution deoxygenated by placing under vacuum and backfilling with nitrogen five times. Tris(dibenzylideneacetone)dipalladium(0) (29 mg, 30 μ mol) was added, the solution was deoxygenated by placing under vacuum and backfilling with nitrogen five times before being heated at 110 °C for 40 h. The mixture was cooled, filtered through a plug of silica using dichloromethane as eluent, and the solvent removed. The residue was purified by column chromatography over silica in two steps: first, using a dichloromethane : light petroleum mixture (2 : 3 to 1 : 1) as eluent, and second, using a benzene : light petroleum mixture (1 : 1 to 13 : 7) as eluent to give **11** as a yellow powder (136 mg, 34%): mp >280 °C (Found: C, 88.4%; H, 6.5%; N, 3.3%. $C_{741}H_{651}IrN_{24}$ requires C, 88.25%;

H, 6.5%; N, 3.3%); $\lambda_{\text{max}}(\text{CH}_2\text{Cl}_2)$ 273 nm (log $\epsilon/\text{dm}^3 \text{ mol}^{-1} \text{ cm}^{-1}$ 5.67), 310sh (5.88), 319 (5.93), 400sh (3.85), 443sh (3.39), 480sh (2.98); $\delta_{\text{H}}(400 \text{ MHz}, \text{CD}_2\text{Cl}_2)$ 0.52–0.77 (240 H, bm, CH_3 and CH_2CH_3), 1.87–2.07 (96, m, $\text{CH}_2\text{CH}_2\text{CH}_3$), and 7.21–7.36, 7.52–7.57, 7.60–7.79, 8.27–8.37, 8.42–8.57, 8.71 (315 H, LigH, CarbH, FIH); m/z [MALDI: DCTB] Anal. Calcd for $\text{C}_{741}\text{H}_{651}\text{IrN}_{24}$: 10077. Found: 10090 (broad) (M^+). GPC: $\bar{M}_w = 6175$, $\bar{M}_v = 6065$, PD = 1.1.

Acknowledgements

We thank the EPSRC for financial support. We also thank the EPSRC National Service for Computational Chemistry Software (URL: <http://www.nscs.ac.uk>) and the APAC National Facility (Canberra, Australia) for computer time, and the EPSRC National Spectroscopy Centre, Swansea, UK. Professor Paul L. Burn is the recipient of an Australian Research Council Federation Fellowship (project number FF0668728).

References

- 1 Y. You, C.-G. An, J.-J. Kim and S.-Y. Park, *J. Org. Chem.*, 2007, **72**, 6241.
- 2 Z. L. Lu, K. Q. Xing, C. P. Luo, Y. Liu, Y. P. Yang, Q. Gan, M. X. Zhu, C. Y. Jiang, Y. Cao and W. G. Zhu, *Chem. Lett.*, 2006, **35**, 538.
- 3 M. A. Baldo, S. Lamansky, P. E. Burrows, M. E. Thompson and S. R. Forrest, *Appl. Phys. Lett.*, 1999, **75**, 4.
- 4 M. Ikai, S. Tokito, Y. Sakamoto, T. Suzuki and Y. Taga, *Appl. Phys. Lett.*, 2001, **79**, 156.
- 5 T. Watanabe, E. Nakamura, S. Kawami, Y. Fukuda, T. Tsuji, T. Wakimoto, S. Miyaguchi, M. Yahiro, M. J. Yang and T. Tsutsui, *Synth. Met.*, 2001, **122**, 203.
- 6 X. Zhou, D. S. Qin, M. Pfeiffer, J. Blochwitz-Nimoth, A. Werner, J. Dreschel, B. Maennig, K. Leo, M. Bold, P. Erk and H. Hartmann, *Appl. Phys. Lett.*, 2002, **81**, 4070.
- 7 X. H. Yang and D. Neher, *Appl. Phys. Lett.*, 2004, **84**, 2476.
- 8 M. Velusamy, K. R. J. Thomas, C.-H. Chen, J. T. Lin, Y. S. Wen, W.-T. Hsieh, C.-H. Lai and P.-T. Chou, *Dalton Trans.*, 2007, 3025.
- 9 X. H. Li, Z. Chen, Q. Zhao, L. Shen, F. Y. Li, T. Yi, Y. Cao and C. H. Huang, *Inorg. Chem.*, 2007, **46**, 5518.
- 10 R. N. Bera, N. Cumpstey, P. L. Burn and I. D. W. Samuel, *Adv. Funct. Mater.*, 2007, **17**, 1149.
- 11 N. Cumpstey, R. N. Bera, P. L. Burn and I. D. W. Samuel, *Macromolecules*, 2005, **38**, 9564.
- 12 P. L. Burn, S.-C. Lo and I. D. W. Samuel, *Adv. Mater.*, 2007, **19**, 1675.
- 13 S.-C. Lo and P. L. Burn, *Chem. Rev.*, 2007, **107**, 1097.
- 14 S.-C. Lo, N. A. H. Male, J. P. J. Markham, S. W. Magennis, P. L. Burn, O. V. Salata and I. D. W. Samuel, *Adv. Mater.*, 2002, **14**, 975.
- 15 T. D. Anthopoulos, M. J. Frampton, E. B. Namdas, P. L. Burn and I. D. W. Samuel, *Adv. Mater.*, 2004, **16**, 557.
- 16 S.-C. Lo, G. J. Richards, J. P. J. Markham, E. B. Namdas, S. Sharma, P. L. Burn and I. D. W. Samuel, *Adv. Funct. Mater.*, 2005, **15**, 1451.
- 17 E. B. Namdas, T. D. Anthopoulos, I. D. W. Samuel, M. J. Frampton, S.-C. Lo and P. L. Burn, *Appl. Phys. Lett.*, 2005, **86**, 161104.
- 18 S.-C. Lo, T. D. Anthopoulos, E. B. Namdas, P. L. Burn and I. D. W. Samuel, *Adv. Mater.*, 2005, **17**, 1945.
- 19 J. C. Ribierre, S. G. Stevenson, I. D. W. Samuel, S. V. Staton and P. L. Burn, *J. Display Technol.*, 2007, **3**, 233.
- 20 B.-L. Li, L. Wu, Y.-M. He and Q.-H. Fan, *Dalton Trans.*, 2007, 2048.
- 21 Y. Q. Li, A. Rizzo, M. Salerno, M. Mazzeo, C. Huo, Y. Wang, K. C. Li, R. Cingolani and G. Gigli, *Appl. Phys. Lett.*, 2006, **89**, 061125.
- 22 T.-H. Kwon, M.-K. Kim, J. Kwon, D.-Y. Shin, S.-J. Park, C.-L. Lee, J.-J. Kim and J.-I. Hong, *Chem. Mater.*, 2007, **19**, 3673.
- 23 J. Q. Ding, J. Gao, Y. X. Cheng, Z. Y. Xie, L. X. Wang, D. G. Ma, X. B. Jing and F. S. Wang, *Adv. Funct. Mater.*, 2006, **16**, 575.
- 24 S.-C. Lo, E. B. Namdas, C. P. Shipley, J. P. J. Markham, T. D. Anthopoulos, P. L. Burn and I. D. W. Samuel, *Org. Electron.*, 2006, **7**, 85.
- 25 N. Iguchi, Y.-J. Pu, K. Nakayama and J. Kido, *J. Photopolym. Sci. Technol.*, 2007, **20**, 73.
- 26 S.-C. Lo, E. B. Namdas, P. L. Burn and I. D. W. Samuel, *Macromolecules*, 2003, **36**, 9721.
- 27 K. R. J. Thomas, J. T. Lin, Y.-T. Tao and C.-W. Ko, *J. Am. Chem. Soc.*, 2001, **123**, 9404.
- 28 I. D. W. Samuel, P. L. Burn and S.-C. Lo, Pat. Appl. GB0222268.5, 2002.
- 29 M. E. Wright and M.-J. Jin, *J. Org. Chem.*, 1989, **54**, 965.
- 30 P. L. Burn, R. Beavington, M. J. Frampton, J. N. G. Pillow, M. Halim, J. M. Lupton and I. D. W. Samuel, *Mater. Sci. Eng., B*, 2001, **85**, 190.
- 31 J. P. J. Markham, I. D. W. Samuel, S.-C. Lo, P. L. Burn, M. Weiter and H. Bässler, *J. Appl. Phys.*, 2004, **95**, 438.
- 32 J. C. Ribierre, A. Ruseckas, K. Knights, S. V. Staton, N. Cumpstey, P. L. Burn and I. D. W. Samuel, *Phys. Rev. Lett.*, 2008, **100**, 017402.
- 33 E. B. Namdas, A. Ruseckas, I. D. W. Samuel, S.-C. Lo and P. L. Burn, *J. Phys. Chem. B*, 2004, **108**, 1570.
- 34 V. V. Grushin, N. Herron, D. D. LeCloux, W. J. Marshall and V. A. Petrov, *Chem. Commun.*, 2001, 1494.
- 35 G. Gritzner and J. Kuta, *Electrochim. Acta*, 1984, **29**, 869.
- 36 J. N. Demas and G. A. J. Crosby, *J. Phys. Chem.*, 1971, **75**, 991.
- 37 M. J. Frisch, G. W. Trucks, H. B. Schlegel, G. E. Scuseria, M. A. Robb, J. R. Cheeseman, J. A. Montgomery Jr, T. Vreven, K. N. Kudin, J. C. Burant, J. M. Millam, S. S. Lyengar, J. Tomasi, V. Barone, B. Mennucci, M. Cossi, G. Scalmani, N. Rega, G. A. Petersson, H. Nakatsuji, M. Hada, M. Ehara, K. Toyota, R. Fukuda, J. Hasegawa, M. Ishida, T. Nakajima, Y. Honda, O. Kitao, H. Nakai, M. Klene, X. Li, J. E. Knox, H. P. Hratchian, J. B. Cross, C. Adamo, J. Jaramillo, R. Gomperts, R. E. Stratmann, O. Yazyev, A. J. Austin, R. Cammi, C. Pomelli, J. W. Ochterski, P. Y. Ayala, K. Morokuma, G. A. Voth, P. Salvador, J. J. Dannenberg, V. G. Zakrzewski, S. Dapprich, A. D. Daniels, M. C. Strain, O. Farkas, D. K. Malick, A. D. Rabuck, K. Raghavachari, J. B. Foresman, J. V. Ortiz, Q. Cui, A. G. Baboul, S. Clifford, J. Cioslowski, B. B. Stefanov, G. Liu, A. Liashenko, P. Piskorz, I. Komaromi, R. L. Martin, D. J. Fox, T. Keith, M. A. Al-Laham, C. Y. Peng, A. Nanayakkara, M. Challacombe, P. M. W. Gill, B. Johnson, W. Chen, M. W. Wong, C. Gonzalez and J. A. Pople, *Gaussian 03, revision C.01 or E.01*, Gaussian, Inc., Wallingford, CT, 2004.
- 38 T. H. Dunning Jr and P. J. Hay, in *Modern Theoretical Chemistry*, ed. H. F. Schaefer, III, Plenum, New York, 1976, vol. 3, p. 1.
- 39 P. J. Hay and W. R. Wadt, *J. Chem. Phys.*, 1985, **82**, 270.
- 40 P. J. Hay and W. R. Wadt, *J. Chem. Phys.*, 1985, **82**, 284.
- 41 P. J. Hay and W. R. Wadt, *J. Chem. Phys.*, 1985, **82**, 299.
- 42 A. D. Becke, *J. Chem. Phys.*, 1993, **98**, 5648.
- 43 S. I. Gorlesky, *AOMix: Program for Molecular Orbital Analysis*, York University, Toronto, Canada, 1997. Available from: <http://www.sg-chem.net>.
- 44 S. I. Gorlesky and A. B. P. Lever, *J. Organomet. Chem.*, 2001, **635**, 187.
- 45 R. Stowasser and R. Hoffmann, *J. Am. Chem. Soc.*, 1999, **121**, 3414.
- 46 A. Vazquez-Mayagoitia, R. Vargas, J. A. Nichols, P. Fuentealba and J. Garza, *Chem. Phys. Lett.*, 2006, **419**, 207.
- 47 W. Yang, H. Y. Zhen, C. Y. Jiang, L. J. Su, J. X. Jiang, H. H. Shi and Y. Cao, *Synth. Met.*, 2005, **153**, 189.